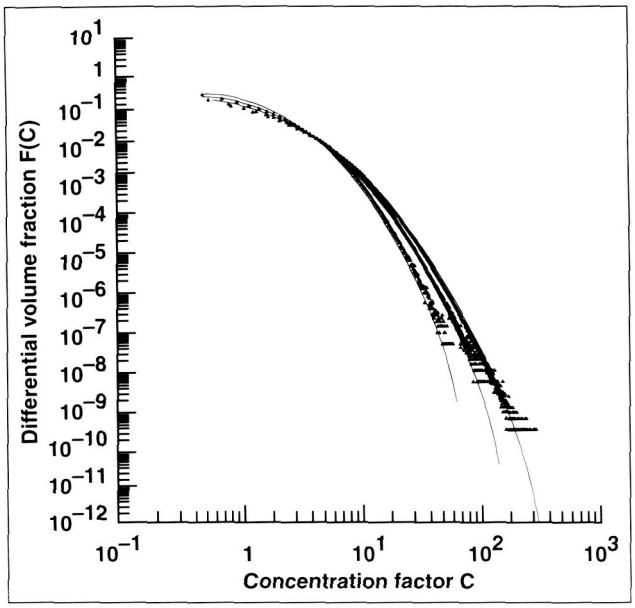

Fig. 2. Comparison of theoretical predictions of volume per unit volume occupied by particles with concentration factor C (lines) with actual binned probability distribution functions. The predictions used only the single fractal descriptor known as the singularity spectrum, which was defined by averaging over data at all three Reynolds numbers. The multifractal approach makes very good predictions of this and other quantities related to the particle-density field.

"singularity spectrum" is determined from the fractal properties of the data). The agreement is very good.

Using this formulation for the nebula, it is predicted that there will be about one clump with a typical dimension of a few kilometers on a side, with a concentration factor of 10^5 to 10^6, for every volume that is 10^4 (1 followed by 4 zeros) kilometers on a side. There will be numerous such clumps in the nebula region of interest, 10^7 kilometers thick and 10^8–10^9 kilometers wide (and even more common concentrations of lower degree). The multifractal formalism is thought to be a fundamental advance in two-phase fluid dynamics; it will be extremely useful in quantitatively describing the properties of selectively concentrated particles in turbulence. For instance, the expected encounter times for chondrules with clumps sufficiently dense to remove the chondrule from circulation, and collision rates within such clumps which augment sticking and accumulation of particles, can also be calculated.

Point of Contact: R. Hogan
(650) 604-0780
hogan@cosmic.arc.nasa.gov

Telltale Electric Currents During Impacts on Rocks

Friedemann Freund, Jerome G. Borucki, Marshall Lisé

Impact studies lead to new insights into geophysical phenomena ranging from electric signals accompanying earthquakes to magnetic signatures of past meteorite impacts on Earth, the Moon, and Mars.

Dry rocks, in particular dry igneous rocks, are known to be good insulators, meaning that they are unable to generate and to transport sizable electric currents. However, evidence has accumulated over the past few years that there is something special about the traces of "water" (H_2O) which nominally anhydrous minerals, the main constituents of igneous rocks, incorporate into their crystal structures when solidifying from water-laden magmas. When water molecules enter a mineral structure, they usually turn into hydroxyls, $H_2O + Si/^{O}\backslash Si = Si/^{OH}{}_{HO}/Si$, but the hydroxyls reshuffle their electrons in such a way that a hydrogen molecule and a peroxy link, $Si/^{OO}\backslash Si$, are formed for each hydroxyl pair.

Since all igneous rocks on Earth and presumably on Mars solidified from water-laden magmas, the presence of peroxy links deserves attention because, when peroxy links can break apart, they generate electric charges. These charges are defect electrons, also known as "positive holes," similar to the holes in semiconductors which are necessary, together with electrons, to build a transistor. Peroxy links dissociate upon heating, but it has now been recognized that they also break apart when subjected to a sudden

mechanical shock. A relatively weak shock suffices; for example, the shock supplied by a steel ball impacting a piece of rock at 100 meters per second. The shock causes the peroxy links to momentarily release positive holes. These act as highly mobile charge carriers and propagate through the mineral structure, jumping from mineral to mineral grain and thus flowing through a rock that would otherwise be considered a good insulator.

To demonstrate the effect, a series of shock-impact experiments was conducted, using for lower velocities a crossbow that can accelerate steel balls up to 100 meters per second, and for higher velocities, 1–6 kilometers per second, the Ames Vertical Gun Range. This paper focuses on the low-velocity impact experiments.

Cylindrical rock cores were fitted with a photodiode for light detection, two capacitive sensors, one at the front near the impact point and one at the far end, and an electrical ground, as shown in the inset in the first part of the figure. When a small steel ball was fired at a velocity of 90 meters per second, the moment of impact manifested itself by a weak, short light pulse, marked by the vertical arrow. Less than 100 microseconds after impact, the front end ring capacitor, about 20 millimeters from the impact point, began to record a positive voltage which eventually rose to +0.5 volt. Another 150 microseconds later, the far-end capacitor (7.5 centimeters downrange) began to record a similar voltage, rising to +50 millivolts, indicating the propagation of a cloud of positive charges at about 300 meters per second. As the front-end capacitor reached +0.5 volt, a second light pulse, much stronger and longer lasting than the first, was emitted from the front end.

In another configuration, depicted in the inset in the second part of the figure, two electrodes were applied to a rectangular piece of the same gabbro (an igneous rock). A photodiode was aimed at the impact point and a pickup coil was installed (not shown) for registering the magnetic field. The electrodes were connected to a 25-volt power supply via a 1-megawatt resistor; the current flowing through this resistor was measured by measuring the voltage

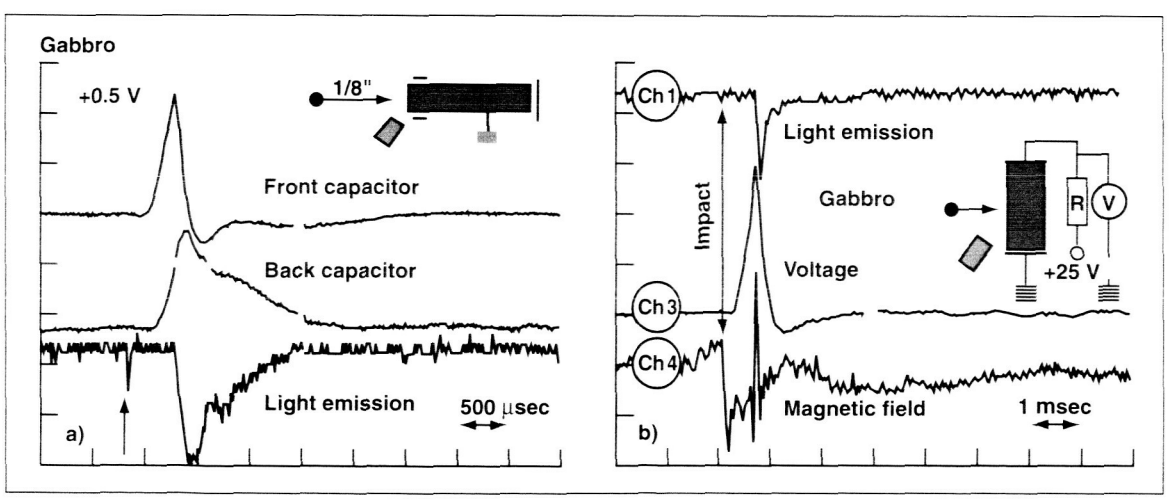

Fig. 1. Example of two low-velocity impacts on gabbro, an igneous rock without piezoelectric quartz. (a) Impact on a cylindrical core resulting in a small light pulse (lower trace, arrow), the appearance of a positive charge, 0.5 volt, at the front-end ring capacitor (upper trace) about 150 microseconds after impact, and after another 150 microseconds of a positive charge at the far-end capacitor (middle trace). Then a strong light pulse occurs from the front end of the rock. (b) Sidewise impact on a rectangular piece of rock with 25 volts applied between two electrodes. The magnetic field pulse (Channel 4) marking the impact is followed by a current of 25 microamperes flowing through the rock (Channel 3) and a strong light pulse (Channel 1) when the current reaches its maximum.

across it. The instant-light emission upon impact was too weak to detect, but the pickup coil registered a magnetic field (Channel 4). After about 125 microseconds the voltage measured across the resistor began to rise (Channel 3), indicating a current of about 25 microamperes. Then the photodiode recorded a sudden light pulse (Channel 1), and the magnetic pickup coil (Channel 4) recorded a brief, but strong magnetic field oscillation.

Point of Contact: F. Freund
(650) 604-5183
ffreund@mail.arc.nasa.gov

Nitrogen Dissociation in Earth's Lower Thermosphere

Winifred M. Huo, Christopher E. Dateo

The reaction of nitrogen atoms (N) with oxygen (O_2) is important in the formation of nitric oxide (NO) in Earth's lower thermosphere. This reaction is particularly sensitive to the internal state of the N atom. The reaction proceeds very slowly if the N atoms are in their ground electronic state (^4S), but becomes much faster for electronically excited N atoms (^2D or ^2P). Thus the amount of NO in the lower thermosphere is dependent on the population of excited-state N atoms. Employing current models of the lower thermosphere, a change in the population of N ^2D from 60% of the total N atom population to 50% results in an 80% decrease in the NO density. Given this uncertainty in the current models, a better understanding of the N atom population distributions is necessary.

Nitrogen atoms in the lower thermosphere are produced by electron impact dissociation of N_2 and the dissociative recombination of N_2^+. Laboratory measurement of electron-impact dissociation of the ground state N_2 ($X^1\Sigma_g^+$) molecule found that equal amounts of ^2D and ^4S nitrogen atoms were produced. This distribution of N atoms gives less ^2D than is used in the model, resulting in an even larger discrepancy between the measured and modeled NO density. To help resolve this discrepancy, large-scale quantum chemical calculations on the dissociation pathways of N_2 have been carried out. The first figure shows

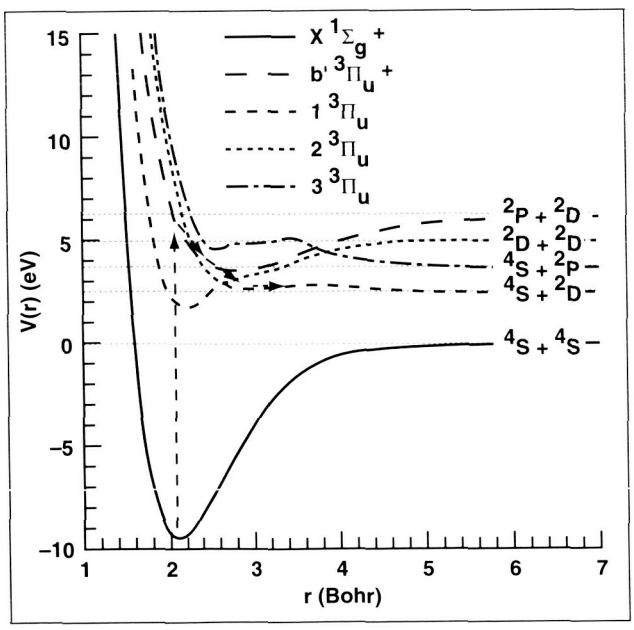

Fig. 1. Dissociation pathways of the $X^1\Sigma_g^+$ state of N_2.

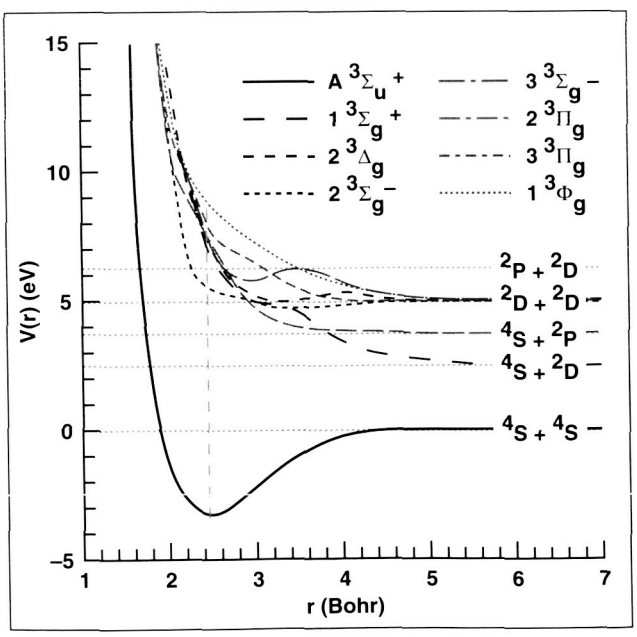

Fig. 2. Dissociation pathways of the $A^3\Sigma_u^+$ state of N_2.